SLAM Using Cellular Multipath Component Delays and Angular Information with JPDA Approximation

Chen, Junshi; Whiton, Russ; Tufvesson, Fredrik

Published in:
2023 8th International Conference on Signal and Image Processing (ICSIP)

DOI:
10.1109/ICSIP57908.2023.10271016

2023

Document Version:
Early version, also known as pre-print

Link to publication

Citation for published version (APA):
Chen, J., Whiton, R., & Tufvesson, F. (2023). SLAM Using Cellular Multipath Component Delays and Angular Information with JPDA Approximation. In *2023 8th International Conference on Signal and Image Processing (ICSIP)* (pp. 973-978). IEEE - Institute of Electrical and Electronics Engineers Inc.. https://doi.org/10.1109/ICSIP57908.2023.10271016

Total number of authors:
3

SLAM Using Cellular Multipath Component Delays and Angular Information with JPDA Approximation

Junshi Chen†*, Russ Whiton†‡, Fredrik Tufvesson†
†Dept. of Electrical and Information Technology, Lund University, Lund, Sweden
*Terranet AB, Lund, Sweden
‡Volvo Car Corporation, SE-405 31 Gothenburg, Sweden
Email: {junshi.chen, russell.whiton, fredrik.tufvesson}@eit.lth.se

***Abstract*—Advanced cellular communication systems provide increased potential for opportunistic high-accuracy positioning. In this paper, long-term evolution (LTE) downlink signals from two commercial base stations (BS) are received by a massive antenna array mounted on a passenger vehicle. Multipath component (MPC) parameters, like delays and angle-of-arrival (AOA) are extracted from the received signals on a snapshot-by-snapshot basis, and then associated across snapshots with a low complexity joint probability data association approximation algorithm. The associated parameters are used to jointly estimate the positions of the vehicle, the transmitters, and the virtual transmitters (VT) with a simultaneous localization and mapping (SLAM) algorithm. Both reflector and scatterer models are adopted, and clock and angular offsets are taken into account in the algorithm. The measurement results show the effectiveness of the data association algorithm and the accuracy of the SLAM algorithm. The vehicle's horizontal position error of SLAM fused with proprioception is less than 5.5 meters after a traversed distance of 530 meters, compared to that of the un-aided proprioception which is 15 meters.**

***Index Terms*—MPC delay, AOA, LTE, massive antenna array, data association, JPDA, integer linear programming, binary tree partition, positioning, localization, SLAM.**

I. Introduction

Cellular communication systems have been widely deployed and achieved tremendous progress in recent years in terms of quality of service and communication speeds. Large bandwidths and granular angular resolution benefit not only communication, but can also enable high accuracy positioning [1], [2]. The natural evolution for such systems is to integrate sensing and communication [3]. This integration can introduce new features to the communication systems themselves, including proactive beam prediction and handover optimization [4], as well as synergize with other systems, e.g., intelligent transport systems, to provide high-accuracy vehicular positioning services [5]–[7].

There are numerous approaches for performing cellular signal-based positioning, which can be categorized as proximity, triangulation, trilateration, fingerprinting (especially machine learning based fingerprinting), hybrid methods, and bayesian filtering based methods like simultaneous localization and mapping (SLAM) [8]. SLAM is a powerful method suitable for online applications in unknown environments or ones with limited resources.

Implementing SLAM entails addressing several challenges. In many cases, data association (DA) is a critical and challenging problem [9]. When the DA is unknown, FastSLAM [10] takes a simple maximum likelihood DA for each particle independently. Only the particles with the highest likelihood of DA with observations can survive the future update. FastSLAM offers low complexity for DA compared to other methods, but it has the drawback of not being able to generate a unified map. Fixed and accurate DA for all particles can not merely provide a unified map, but also increase the effectiveness of SLAM. In order to achieve accurate DA, several advanced algorithms have been developed, e.g., joint probabilistic data association (JPDA) [11], multiple hypothesis tracker (MHT) [12], and graphical model approaches [13], etc. In general, JPDA can find the optimal DA, but it has high complexity even for a relatively large number of measurements, therefore, some low complexity JPDA approximation algorithms have been proposed, see, e.g., [14], [15].

In this paper, downlink signals from multiple commercial long-term evolution (LTE) base stations (BS) are received by a massive antenna array in an urban environment [16]. The multipath component (MPC) parameters, including delays, azimuthal angles-of-arrival (AOA), and elevational AOA, are extracted and employed for positioning. First, the joint probabilistic association (JPDA) of MPC parameters from different snapshots is represented as an integer linear programming (ILP) problem, and the approximation of ILP is achieved by finding the m best association hypotheses with the binary tree partition algorithm. Next, the SLAM algorithm is applied to the associated parameters to find the position of the vehicle, the transmitters, and the virtual transmitters with the fusion of onboard inertial measurement unit (IMU) and wheel odometry. Static but unknown clock offsets between the vehicle and the BSs are assumed, as well as static calibration errors in the antenna array mounting on the vehicle. A SLAM model considering both reflectors and scatterers is adopted. Results from field measurements show that the JPDA approximation can associate MPC parameters accurately and provide good input to SLAM, which works well in the complicated urban environment tested. After traversing 530 meters the horizontal positioning error is less than 5.5 meters.

The structure of the paper is as follows. Sec. II introduces the wireless signal system model. Sec. III describes the

JPDA approximation algorithm associating the estimated MPC parameters from different snapshots, Sec. IV describes the SLAM model using the MPC parameters after association, Sec. V describes the iterative update of the SLAM algorithm applied to localize the position of the vehicle and generate a map of the transmitters and virtual transmitters. Sec. VI presents the measurement setup and analysis of the results from the data association algorithm and the SLAM algorithm. Finally, Sec. VII summarizes the paper.

Notation: Matrices and vectors are denoted as uppercase and lowercase boldface letters, e.g., $\mathbf{A}$ and $\mathbf{a}$. The identity matrix is denoted as $\mathbf{I}$. The matrix transpose and matrix inverse are denoted as superscripts $(\cdot)^T$ and $(\cdot)^{-1}$ respectively. The 1-norm and 2-norm of a vector are denoted as $\|\cdot\|_1$ and $\|\cdot\|_2$ respectively. The speed of light is $c \simeq 3 \cdot 10^8$ m/s.

II. System Model

A 128-port stacked uniform circular antenna array is mounted on a passenger vehicle to receive the LTE signals from multiple commercial base stations simultaneously in urban environments. The channel frequency response from the j-th port of the k-th BS is modeled as a sum of M MPCs which are parameterized by the delay $\tau^{m,j,k}$, direction-of-arrival (DOA) $\Omega^{m,j,k}$, and Doppler shift $\nu^{m,j,k}$. The DOA is further divided into azimuth AOA $\varphi^{m,j,k}$ and elevation AOA $\theta^{m,j,k}$. The time-varying directional transfer function of the n-th subcarrier is represented as

$$\mathbf{h}^{j,k}[n] = \sum_{m=1}^{M} \mathbf{b}_R(\Omega^{m,j,k})\mathbf{\Gamma}^{m,j,k}\mathbf{b}_T^{j,k} e^{-i2\pi(n\Delta f\tau^{m,j,k} - \nu^{m,j,k}t)} \quad (1)$$

where $\mathbf{b}_R(\Omega^{m,j,k}) \in \mathbb{C}^{128\times 2}$ is the receive antenna array pattern, $\mathbf{b}_T^{j,k} \in \mathbb{C}^{2\times 1}$ is the antenna response of the j-th port of the k-th BS, Δf is the subcarrier spacing, and $\mathbf{\Gamma}^{m,j,k}$ is the polarimetric path weight matrix defined as

$$\mathbf{\Gamma}^{m,j,k} = \begin{bmatrix} \gamma_{\mathrm{HH}}^{m,j,k} & \gamma_{\mathrm{VH}}^{m,j,k} \\ \gamma_{\mathrm{HV}}^{m,j,k} & \gamma_{\mathrm{VV}}^{m,j,k} \end{bmatrix}. \quad (2)$$

The matrix elements represent different polarization combinations of the transmitter and the receiver antenna, e.g., HV is horizontal-to-vertical.

The received common reference signal (CRS) [17] in the frequency domain of the n-th subcarrier is given as follows

$$\mathbf{y}[n] = \sum_{k=1}^{K}\sum_{j=1}^{J} \mathbf{h}^{j,k}[n] \cdot x_{CRS}^{j,k}[n] \quad (3)$$

here $x_{CRS}^{j,k}[n]$ is the CRS signal from the j-th antenna port of the k-th BS at the n-th subcarrier.

Due to the presence of multiple BSs with colliding CRS, the interference cancellation method is employed to separate the CRS from the same antenna port of different BSs. Next, the modified RIMAX algorithm is utilized to extract the MPC parameters including delay, azimuth AOA, and elevation AOA as described in [16].

In order to apply the estimated MPC delays to positioning, they are converted into the distance domain by adding the clock offset t_{offset}^k between the k-th BS and the vehicle, which is treated as an unknown constant, and multiplied by the speed of light

$$d_t^{m,j,k} = \left(\tau_t^{m,j,k} + t_{\mathrm{offset}}^k\right) \cdot c. \quad (4)$$

The MPCs' parameters at time index t can be grouped as

$$\mathbf{S}_t = \left[\mathbf{s}_t^{1,1,1}, \ldots, \mathbf{s}_t^{M,J,K}\right] \quad (5)$$

$$\mathbf{s}_t^{m,j,k} = \left[d_t^{m,j,k}, \varphi_t^{m,j,k}, \theta_t^{m,j,k}\right]^T. \quad (6)$$

III. Low complexity joint probabilistic data association approximation

After the MPC parameters at each snapshot are estimated, they need to be associated among different snapshots. JPDA is a traditional method for DA with high computational complexity, and it can be approximated by utilizing the ILP with low complexity as shown in [14].

Let $z_t^1, \ldots, z_t^N$ be the states of all the targets, and $s_t^1, \ldots, s_t^M$ be the measurements from one cell ID at time index t. The term $p_t(c_i^j = 1)$ (denoted as $p_t(c_i^j)$) represents the probability of associating the measurement $s_t^i, i \in \{0, 1, ..., M\}$ with the target $z_t^j, j \in \{1, ..., N\}$ at time index t. Here the index 0 represents a missed detection. The probability $p_t(c_i^j)$ is defined as

$$p_t(c_i^j) \propto \begin{cases} (1-p_d)p_{fa} & \text{if } i = 0 \\ p_d \cdot \mathcal{N}(s_t^i; \hat{z}_t^j, \Sigma_s) & \text{otherwise} \end{cases} \quad (7)$$

where p_d is the detecting probability, p_{fa} is the false alarm probability, $\mathcal{N}$ is the normal distribution, $\hat{z}_t^j$ is the predicted position of the j-th target at time index t and Σ_s is the covariance matrix of the target.

The JPDA algorithm calculates the marginalized probability $g_t(c_i^j = 1)$ (denoted as $g_t(c_i^j)$) on the joint data association space Ψ that has all the possible associations between the measurements and the targets based on the assumption that:

- Each measurement (except the one with index 0) originates from at most one target;
- Each target generates at most one unique measurement.

The space Ψ can be represented as

$$\Psi = \Bigg\{\psi = (c_i^j)_{i\in[M], j\in[N]} \mid c_i^j \in \{0,1\} \\ \& \sum_{j=1}^{N} c_i^j \leq 1, \forall i \in [M] \,\&\, \sum_{i=1}^{M} c_i^j = 1, \forall j \in [N]\Bigg\}. \quad (8)$$

The element $\Psi_i^j \subset \Psi$ includes all the associations that map the j-th target to the i-th measurement, i.e., $\Psi_i^j = \{\psi \in \Psi \mid c_i^j = 1\}$, then $g_t(c_i^j)$ is achieved by marginalizing over the subset Ψ_i^j as

$$g_t(c_i^j) = \sum_{\psi\in\Psi_i^j} p(\psi) \quad (9)$$

where

$$p(\psi) = \prod_{\substack{\forall r\in[M] \\ \forall k\in[N]}} \left(p_t(c_r^k)\right)^{c_r^k} \quad (10)$$

The data association problem can be rewritten as a minimization problem as

$$f_1^\star = \min_{\psi\in\Psi} -\log\left(p(\psi)\right) = \sum_{\substack{\forall r\in[M]\\ \forall k\in[N]}} -\left(\log\left(p_t(c_r^k)\right)\cdot c_r^k\right)$$

$$\text{s. t.} \sum_{k=1}^{N} c_r^k \leq 1 \ \forall r\in[M] \ \& \ \sum_{r=0}^{M} c_r^k = 1 \ \forall k\in[N]. \quad (11)$$

It can be reformulated as an ILP problem [18]

$$f_1^\star = \min_{c\in\{0,1\}^n} \mathbf{f}^T\mathbf{c} \quad \text{s.t.} \quad \mathbf{Ac}\leq\mathbf{b} \quad (12)$$

here $\mathbf{c}=[c_1,\ldots,c_n]^T$ is a binary vector of length of $N(M+1)$ so that $c_l = c_r^k$, $f=[f_1,\ldots,f_n]^T$ is the cost vector so that $f_l = -\log(p_t(c_r^k))$, and the matrix $\mathbf{A}$ and the vector $\mathbf{b}$ are defined to satisfy the constrains in eq. (11) as shown in [14].

The hypotheses space between the targets and the measurements is huge when the number of targets and measurements is relatively large, which results in high computation complexity for JPDA, but it can be approximated by taking only a small subset of the space Δ_i^j that contains the hypotheses with highest probabilities, so that

$$g_t(c_i^j) \approx \sum_{\psi\in\Delta_i^j} p\left(\psi\right) \quad (13)$$

which is equivalent to finding m best solutions that fulfill eq. (12). The first solution and the m-th best solution of eq. (12) can be represented respectively as

$$\mathbf{c}^1 = \arg\min_{\mathbf{c}} \mathbf{f}^T\mathbf{c} \text{ s.t. } \mathbf{Ac}\leq\mathbf{b} \quad (14)$$

$$\mathbf{c}^m = \arg\min_{\mathbf{c}} \mathbf{f}^T\mathbf{c} \text{ s.t. } \begin{cases}\mathbf{Ac}\leq\mathbf{b}\\ \forall k<m, \langle\mathbf{c},\mathbf{c}^k\rangle < \left\|\mathbf{c}^k\right\|_1\end{cases} \quad (15)$$

In order to find all the m best solutions to approximate the JPDA assignment probability of eq. (13), a low complexity binary tree partition method is adopted in [14], which iteratively solves a series of constrained second-best problems. The detailed algorithm is shown in Algorithm 1.

After all the m best solutions are found, the targets can be updated by combining the associated measurements with corresponding probabilities. If a measurement has all the associated probabilities lower than a threshold, then it is considered a new target and initialized, similarly, if a target has all the associated probabilities lower than a threshold, then it is considered a missed detection.

IV. SLAM MODEL USING THE ASSOCIATED MPC PARAMETERS

MPCs from the same BS with line-of-sight (LOS), or reflected and scattered by the environment with non line-of-sight (NLOS) are considered as synchronized and independent transmitters and virtual transmitters (VT) respectively [19]. The term VT is used to refer to all the transmitters for representation convenience. The motivation of SLAM is to fuse wireless signals and onboard sensors to accurately estimate

input : $\mathbf{f},\mathbf{A},\mathbf{b},m$

output: $\mathbf{c}^{(k)}, k=1,\ldots,m$

$\mathbf{c}^1 = \arg\min_{\mathbf{c}} \mathbf{f}^T\mathbf{c}$ s.t. $\mathbf{Ac}\leq\mathbf{b}$;

$\mathbf{c}^2 = \arg\min_{\mathbf{c}} \mathbf{f}^T\mathbf{c}$ s.t. $\mathbf{Ac}\leq\mathbf{b}, \langle\mathbf{c},\mathbf{c}^1\rangle < \left\|\mathbf{c}^1\right\|_1$;

Select arbitary $j\in\{i \mid c_i^1 \neq c_i^2\}$;

$\mathcal{F}_3^1 = \{\mathbf{c}\in\mathbb{B}^n \mid \mathbf{Ac}\leq\mathbf{b}, \langle\mathbf{c},\mathbf{c}^1\rangle < \left\|\mathbf{c}^1\right\|_1, c_j = c_j^1\}$;

$\mathcal{F}_3^2 = \{\mathbf{c}\in\mathbb{B}^n \mid \mathbf{Ac}\leq\mathbf{b}, \langle\mathbf{c},\mathbf{c}^2\rangle < \left\|\mathbf{c}^2\right\|_1, c_j = c_j^2\}$;

$\mathbf{c}_3^1 = \arg\min_{\mathbf{c}\in\mathcal{F}_3^1} \mathbf{f}^T\mathbf{c}$;

$\mathbf{c}_3^2 = \arg\min_{\mathbf{c}\in\mathcal{F}_3^2} \mathbf{f}^T\mathbf{c}$;

for $k=3$ *to* m **do**

  $l_k = \arg\min_l \mathbf{f}^T\mathbf{c}_k^l, \mathbf{c}^k = \mathbf{c}_k^{l_k}$;

  $\mathcal{F}_{k+1}^l = \mathcal{F}_k^l, c_{k+1}^l = c_k^l, \forall l<k, l\neq l_k$;

  Select arbitary $j_k\in\{i \mid c_i^{l_k} \neq c_i^k\}$;

  $\mathcal{F}_{k+1}^{l_k} = \mathcal{F}_k^{l_k} \cap \{\mathbf{c} \mid \langle\mathbf{c},\mathbf{c}^{l_k}\rangle < \left\|\mathbf{c}^{l_k}\right\|_1, c_{j_k} = c_{j_k}^{l_k}\}$;

  $\mathcal{F}_{k+1}^{k} = \mathcal{F}_k^{l_k} \cap \{\mathbf{c} \mid \langle\mathbf{c},\mathbf{c}^{k}\rangle < \left\|\mathbf{c}^{k}\right\|_1, c_{j_k} = c_{j_k}^{k}\}$;

  Remove constraints $\langle\mathbf{c},\mathbf{c}^{l_k}\rangle < \left\|\mathbf{c}^{l_k}\right\|_1$ from $\mathcal{F}_{k+1}^{l_k}$;

  Remove constraints $\langle\mathbf{c},\mathbf{c}^{k}\rangle < \left\|\mathbf{c}^{k}\right\|_1$ from $\mathcal{F}_{k+1}^{k}$;

  $\mathbf{c}_{k+1}^l = \arg\min_{\mathbf{c}\in\mathcal{F}_{k+1}^l} \mathbf{f}^T\mathbf{c}$, for $l\in\{l_k,k\}$;

end

Algorithm 1: Binary tree partition to approximate JPDA

the position of the vehicle and provide a high-precision map of VTs. The posterior can be represented as

$$p\left(\mathbf{V},\mathbf{r}_{1:t} \mid \mathbf{Z}_{1:t},\mathbf{u}_{1:t}\right) \quad (16)$$

here $\mathbf{V}$ represents the positions of the VTs, $\mathbf{r}_{1:t}$ is the time series of the vehicle state vector, $\mathbf{Z}_{1:t}$ are the associated parameters, and $\mathbf{u}_{1:t}$ is the input velocity from other sensors of the vehicle. The index $1:t$ represents the time from time index 1 to t.

The positions of the VTs are given as

$$\mathbf{V} = \left[\mathbf{v}^{1,1,1,1},\ldots,\mathbf{v}^{L,M,J,K}\right] \quad (17)$$

$$\mathbf{v}^{l,m,j,k} = \left[v_x^{l,m,j,k}, v_y^{l,m,j,k}, v_z^{l,m,j,k}, d^{l,m,j,k}\right]^T \quad (18)$$

here $\mathbf{v}^{l,m,j,k}$ is the position status vector of the VT from the m-th MPC of the j-th antenna port of the k-th BS. $\left[v_x^{l,m,j,k}, v_y^{l,m,j,k}, v_z^{l,m,j,k}\right]$ is the position of the VT in Cartesian coordinates, and $d^{l,m,j,k}$ is the distance between the BS and the scatterer. Here the scattering model from [19] is adopted and one MPC is represented by L particles with different scatterer distances.

The vehicle's state vector can be represented as

$$\mathbf{r}_{1:t} = \left[\mathbf{r}_1,\ldots,\mathbf{r}_t\right] \quad (19)$$

$$\mathbf{r}_t = \left[r_x(t), r_y(t), r_z(t), r_\psi(t), r_\theta(t), r_\phi(t), d_o^k, \varphi_o, \theta_o\right]^T \quad (20)$$

where $\mathbf{r}_p(t) = [r_x(t), r_y(t), r_z(t)]^T$ is the vehicle's position in Cartesian coordinates at time index t, $[r_\psi(t), r_\theta(t), r_\phi(t)]$ are the vehicle's yaw, pitch, and roll, d_o^k is the distance offset caused by the clock offset t^k_{offset}, φ_o and θ_o are the azimuthal and elevational offset between the antenna array coordinates and the vehicle coordinates due to calibration error.

The vehicle's velocity $\mathbf{u}_t$ includes longitudinal, lateral, vertical, yaw, pitch, and roll velocities. Rotational velocities are available from the IMU, and longitudinal speed is available from the wheel odometry. The velocity can be represented as

$$\mathbf{u}_t = [u_x, u_y, u_z, u_\psi, u_\theta, u_\phi]^T . \tag{21}$$

The SLAM algorithm with known data association in [19] is adopted to solve the posterior problem, and it can decompose the posterior into a factored form with the Rao-Blackwellization algorithm [20] as

$$\begin{aligned} &p\left(\mathbf{V}, \mathbf{r}_{1:t} \mid \mathbf{Z}_{1:t}, \mathbf{u}_{1:t}\right) = \\ &p\left(\mathbf{r}_{1:t} \mid \mathbf{Z}_{1:t}, \mathbf{u}_{1:t}\right) \prod_{n\in\{M,J,K\}} \sum_{l=1}^{L} p\left(\mathbf{v}^{l,n} \mid \mathbf{r}_{1:t}, \mathbf{Z}_{1:t}\right). \end{aligned} \tag{22}$$

Since the MPCs from different antenna ports and different BSs are conditionally independent and separable by cell ID, the posterior can be further factored as

$$\begin{aligned} &p\left(\mathbf{V}, \mathbf{r}_{1:t} \mid \mathbf{Z}_{1:t}, \mathbf{u}_{1:t}\right) = p\left(\mathbf{r}_{1:t} \mid \mathbf{Z}_{1:t}, \mathbf{u}_{1:t}\right) \\ &\prod_{k=1}^{K}\prod_{j=1}^{J}\prod_{m=1}^{M}\sum_{l=1}^{L} p\left(\mathbf{v}^{l,m,j,k} \mid \mathbf{r}_{1:t}, \mathbf{z}^{m,j,k}_{1:t}\right) \end{aligned} \tag{23}$$

where $\mathbf{z}^{m,j,k}_{1:t}$ represents the associated parameters of the m-th MPC from the j-th antenna port of the k-th BS. This method can process the position estimation of VTs from different associated MPCs, antenna ports, and BSs separately with low complexity and high flexibility.

V. SLAM update with the associated MPC parameters

The vehicle's status $\mathbf{r}_t$ at time index t is a function of control inputs $\mathbf{u}_t$ and pose state $\mathbf{r}_{t-1}$ of previous time index $t-1$, and it is described in the motion model as

$$p(\mathbf{r}_t \mid \mathbf{r}_{t-1}, \mathbf{u}_t). \tag{24}$$

A particle filter is adopted to estimate the vehicle's posterior. At each time index, it keeps a set of particles representing the posterior $p(\mathbf{r}_{1:t} \mid \mathbf{Z}_{1:t}, \mathbf{u}_{1:t})$, and the set is denoted as $\mathbf{R}_{1:t}$. Each particle $\mathbf{r}_{i,1:t}$ represents the i-th hypothesis of the vehicle's path, i.e.,

$$\mathbf{R}_{1:t} = \{\mathbf{r}_{i,1:t}\}_i = \{\mathbf{r}_{i,1}, \ldots, \mathbf{r}_{i,t}\}_i \tag{25}$$

here each particle is assumed to have unique and constant values of $d^k_{i,o}, \varphi_{i,o}$ and $\theta_{i,o}$ among the offset ranges.

The probabilistic hypothesis of the vehicle's pose $\mathbf{r}_{i,t}$ at time index t is generated by sampling the particle $\mathbf{r}_{i,t-1}$ at time index $t-1$ from the probabilistic motion model

$$\mathbf{r}_{i,t} \sim p\left(\mathbf{r}_t \mid \mathbf{r}_{i,t-1}, \mathbf{u}_t\right). \tag{26}$$

After all the vehicle's particles are generated, the SLAM algorithm updates the posterior of the VT estimates associated with each particle. For a VT connected to the i-th vehicle particle, its posterior corresponding to the l-th particle at the time index t is updated as follows

$$\begin{aligned} &p(\mathbf{v}^{l,m,j,k}_i \mid \mathbf{r}_{i,1:t}, \mathbf{z}^{m,j,k}_{1:t}) = \\ &\eta p(\mathbf{z}^{m,j,k}_t \mid \mathbf{r}_{i,t}, \mathbf{v}^{l,m,j,k}_i) p(\mathbf{v}^{l,m,j,k}_i \mid \mathbf{r}_{i,1:t-1}, \mathbf{z}^{m,j,k}_{1:t-1}) \end{aligned} \tag{27}$$

here η is the normalization factor, and the posterior of $\mathbf{v}^{l,m,j,k}_i$ at the time index $t-1$ is assumed to be Gaussian with the mean and variance as follows

$$p\left(\mathbf{v}^{l,m,j,k}_i \mid \mathbf{r}_{i,1:t-1}, \mathbf{z}^{m,j,k}_{1:t-1}\right) \sim \mathcal{N}\left(\boldsymbol{v}^{l,m,j,k}_i; \boldsymbol{\mu}^{l,m,j,k}_{i,t-1}, \boldsymbol{\Sigma}^{l,m,j,k}_{i,t-1}\right). \tag{28}$$

In order to ensure that the estimate of VT at the time index t is Gaussian, the perceptual model $p(\mathbf{z}^{m,j,k}_t \mid \mathbf{r}_{i,t}, \mathbf{v}^{l,m,j,k}_i)$ is linearized, and the measurement function can be approximated through Taylor expansion as

$$h(\mathbf{v}^{l,m,j,k}_i, \mathbf{r}_{i,t}) = \hat{\mathbf{z}}^{l,m,j,k}_{i,t} + \mathbf{H}^{l,m,j,k}_{i,t}(\mathbf{v}^{l,m,j,k}_i - \boldsymbol{\mu}^{l,m,j,k}_{i,t-1}) \tag{29}$$

$$\hat{\mathbf{z}}^{l,m,j,k}_{i,t} = h\left(\boldsymbol{\mu}^{l,m,j,k}_{i,t-1}, \mathbf{r}_{i,t}\right) \tag{30}$$

where the function h is a set of equations to estimate the distance, azimuth AOA, and elevation AOA from the positions of the vehicle and the VT, and $\mathbf{H}^{l,m,j,k}_{i,t}$ is the Jacobian of h. The function h is constituted by the following equations

$$\hat{d}^{l,m,j,k}_i(t) = \left\|\boldsymbol{\mu}^{l,m,j,k}_{i,t-1} - \mathbf{r}_{i,p}(t)\right\|_2 + d^{l,m,j,k} + d^k_{i,o} \tag{31}$$

$$\hat{\varphi}^{l,m,j,k}_i(t) = \text{atan}\left(\frac{\hat{y}}{\hat{x}}\right) + \varphi_{i,o} \tag{32}$$

$$\hat{\theta}^{l,m,j,k}_i(t) = \text{asin}\left(\frac{\sqrt{\hat{x}^2 + \hat{y}^2}}{\hat{z}}\right) + \theta_{i,o} \tag{33}$$

here $[\hat{x}, \hat{y}, \hat{z}]^T$ is achieved according to Euler's rotation theorem [21]

$$[\hat{x}, \hat{y}, \hat{z}]^T = \mathbf{R}\left(r_{i,\psi}(t), r_{i,\theta}(t), r_{i,\phi}(t)\right)\left(\boldsymbol{\mu}^{l,m,j,k}_{i,t-1} - \mathbf{r}_{i,p}(t)\right) \tag{34}$$

and $\mathbf{R}\left(r_{i,\psi}(t), r_{i,\theta}(t), r_{i,\phi}(t)\right)$ is the rotation matrix.

With the linearization, the mean and covariance of each VT at time index t can be updated with the standard extended Kalman filter [22] as follows

$$\mathbf{K}^{l,m,j,k}_{i,t} = \boldsymbol{\Sigma}^{l,m,j,k}_{i,t-1}\mathbf{H}^{l,m,j,k\,T}_{i,t}(\mathbf{H}^{l,m,j,k}_{i,t}\boldsymbol{\Sigma}^{l,m,j,k}_{i,t-1}\mathbf{H}^{l,m,j,k\,T}_{i,t} + \mathbf{Q}_t)^{-1} \tag{35}$$

$$\boldsymbol{\mu}^{l,m,j,k}_{i,t} = \boldsymbol{\mu}^{l,m,j,k}_{i,t-1} + \mathbf{K}^{l,m,j,k}_{i,t}(\mathbf{z}^{m,j,k}_t - \hat{\mathbf{z}}^{l,m,j,k}_{i,t}) \tag{36}$$

$$\boldsymbol{\Sigma}^{l,m,j,k}_{i,t} = (\mathbf{I} - \mathbf{K}^{l,m,j,k}_{i,t}\mathbf{H}^{l,m,j,k}_{i,t})\boldsymbol{\Sigma}^{l,m,j,k}_{i,t-1}. \tag{37}$$

After the posteriors of all the VTs are updated, all the particles' importance factors are calculated and applied proportionally in the resampling of the particles. The i-th particle's importance factor is calculated as follows

$$\begin{aligned} w_{i,t} &= \frac{\text{target distribution}}{\text{proposal distribution}} = \frac{p(\mathbf{r}_{i,1:t} \mid \mathbf{Z}_{1:t}, \mathbf{u}_{1:t})}{p(\mathbf{r}_{i,1:t} \mid \mathbf{Z}_{1:t-1}, \mathbf{u}_{1:t})} \\ &\propto w_{i,t-1}\prod_{k\in K}\prod_{j\in J}\prod_{m\in M}\sum_{l=1}^{L}\tilde{w}^{l,m,j,k}_{i,t-1}\int p\left(\mathbf{z}^{m,j,k}_t \mid \mathbf{r}_{i,t}, \mathbf{v}^{l,m,j,k}_i\right) \\ &p\left(\mathbf{v}^{l,m,j,k}_i \mid \mathbf{r}_{i,1:t-1}, \mathbf{z}^{m,j,k}_{1:t-1}\right) d\mathbf{v}^{l,m,j,k}_i. \end{aligned} \tag{38}$$

The last part in the equation is already defined in eq. (28). With the same linearization as in eq. (29), the importance factor can be calculated as

$$w_{i,t} \propto w_{i,t-1}\prod_{k\in K}\prod_{j\in J}\prod_{m\in M}\sum_{l=1}^{L}\tilde{w}^{l,m,j,k}_{i,t} \tag{39}$$

TABLE I: Measurement system information [16]

Parameter Name	Value
Center frequency	2.66 GHz
System bandwidth	20 MHz
BS number	2
Cell IDs of BS A	375, 376, 377
Cell IDs of BS B	177, 178, 179
Tx antenna port number	2
Rx antenna port number	128
Snapshot interval	75 ms
Total snapshot number	6850
Total test time	8.5 minutes
Traversed distance	530 meters

$$\tilde{w}_{i,t}^{l,m,j,k} = \tilde{w}_{i,t-1}^{l,m,j,k} \left|2\pi \mathbf{Q}_{i,t}^{l,m,j,k}\right|^{-\frac{1}{2}} e^{\left(-\frac{1}{2}\left(\mathbf{z}_t^{m,j,k}-\hat{\mathbf{z}}_{i,t}^{l,m,j,k}\right)^T \left(\mathbf{Q}_{i,t}^{l,m,j,k}\right)^{-1} \left(\mathbf{z}_t^{m,j,k}-\hat{\mathbf{z}}_{i,t}^{l,m,j,k}\right)\right)} \tag{40}$$

and the covariance is

$$\mathbf{Q}_{i,t}^{l,m,j,k} = \left(\mathbf{H}_{i,t}^{m,j,k}\right)^T \mathbf{\Sigma}_{i,t-1}^{m,j,k} \mathbf{H}_{i,t}^{m,j,k} + \mathbf{Q}_t \tag{41}$$

here $\mathbf{Q}_t$ is the covariance matrix of the measurement.

The minimum mean square error (MMSE) estimation of the positions of the vehicle and the VTs is defined as

$$\bar{\mathbf{r}}_t = \sum_i w_{i,t} \cdot \mathbf{r}_{i,t} \tag{42}$$

$$\bar{\mathbf{v}}_t^{m,j,k} = \sum_i w_{i,t} \cdot \sum_{l=1}^{L} \tilde{w}_{i,t}^{l,m,j,k} \cdot \mathbf{v}_i^{l,m,j,k}. \tag{43}$$

VI. Measurement Setup and Results Analysis

A measurement system using USRP to control the switch of the 128-port stacked uniform circular antenna array was developed, and a measurement campaign of receiving commercial LTE signals from multiple BSs was conducted by mounting the system on the roof of a vehicle and driving in the urban area of the city of Lund, Sweden. The parameters are shown in Table I. The 128 receiving antennas were switched in a fixed pattern with a 0.5 ms switching interval. The vehicle moved at a relatively low speed of around 1.0 m/s due to the nature of the switched antenna array system. The ground truth pose was generated using an OXTS RT3003G system. The longitudinal speed was taken from the wheel odometry, and the yaw velocity was retrieved from the IMU. Both sensors were available in the vehicle.

The MPC azimuth AoA estimates from RIMAX for sector 376 of BS A and sector 178 of BS B are shown in Fig. 1 and Fig. 2 respectively. The associated MPC azimuth AoA estimations from the JPDA approximation after pruning the ones with short lifetimes are also shown in the corresponding figures. It can be observed that the JPDA approximation can associate the MPC azimuth AOA estimations accurately and suppress the spurious MPCs effectively.

The measurement trajectory is shown in Fig. 3. It contains the trajectories of ground truth, SLAM, and proprioception. Here SLAM estimation fuses the delays and angular information from the cellular signals, the rotation information from the IMU, and the speed information from the wheel odometry, while proprioception uses the information from the IMU and wheel odometry alone. The estimated positions of the physical reflectors corresponding to VTs from SLAM are calculated, and they are shown in the figure as different color dots. The physical reflectors at 33.8 seconds are shown as stars and corresponding buildings are highlighted. It can be observed that the physical reflectors' positions fit well with the map data.

The absolute error of the estimated vehicle trajectory from SLAM and proprioception only are shown as a function of time in Fig. 4. It can be observed that SLAM with JPDA approximation can improve positioning performance greatly. It has 5.5 meters of maximum

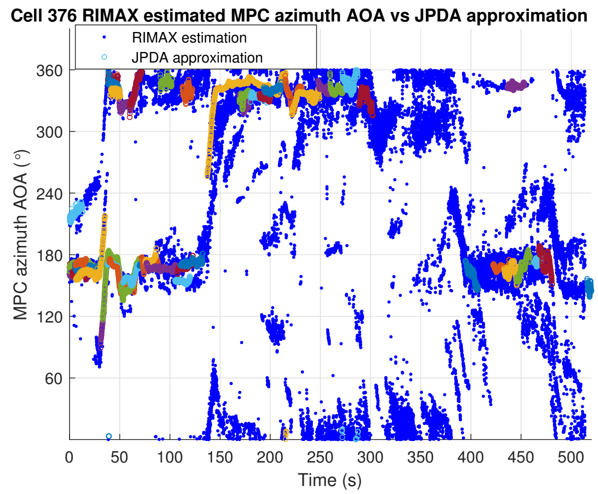

Fig. 1: Cell 376 multipath component azimuth AOA estimated by RIMAX and associated with JPDA approximation.

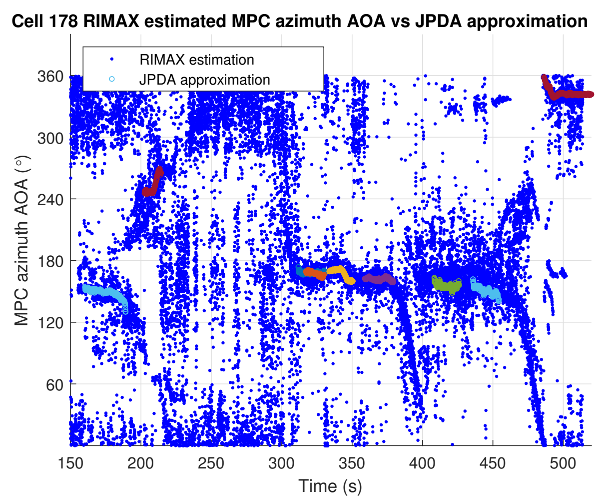

Fig. 2: Cell 178 multipath component azimuth AOA estimated by RIMAX and associated with JPDA approximation.

absolute horizontal error around 270 seconds and has 4 meters of horizontal error at the end after a traversed distance of 530 meters. Proprioception alone has 20 meters of maximum horizontal absolute error and 15 meters of horizontal error at the end of the measurement.

VII. Conclusion

In this paper, multipath component parameters like delays and angular information are used for positioning. These parameters are extracted from the commercial LTE base stations received by the 128-port antenna array in urban environments, associated with the joint probabilistic data association approximation algorithm, which represents the data association as an integer linear programming problem and approximates the solution with binary tree partition effectively. Afterward, the associated multipath component parameters are sent to the SLAM algorithm, which can process the multipath components of each antenna port of each base station independently and consider the reflector and scatterer model with fixed clock and angular offsets between the vehicle and the BSs. The data association results show the accuracy and effectiveness of the adopted algorithm, and the positioning results validate the SLAM algorithm and demonstrate the capability of exploiting LOS and NLOS multipath components for high accuracy positioning in complicated urban environments.

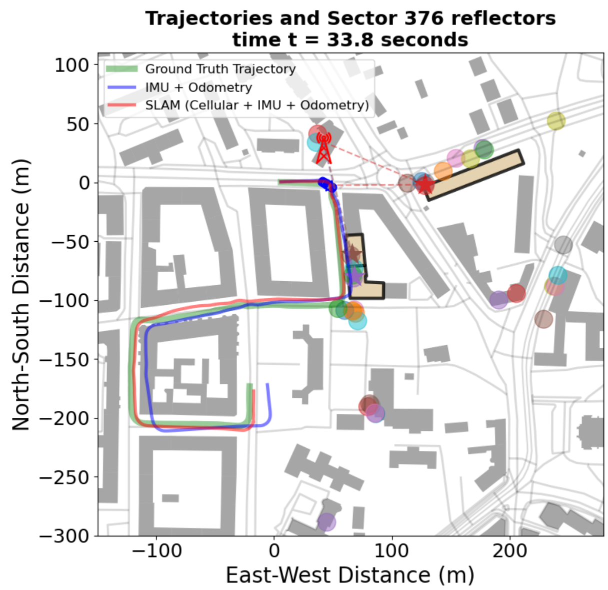

Fig. 3: The ground truth trajectory together with the SLAM estimation and proprioception-only, and the positions of reflectors from one sector.

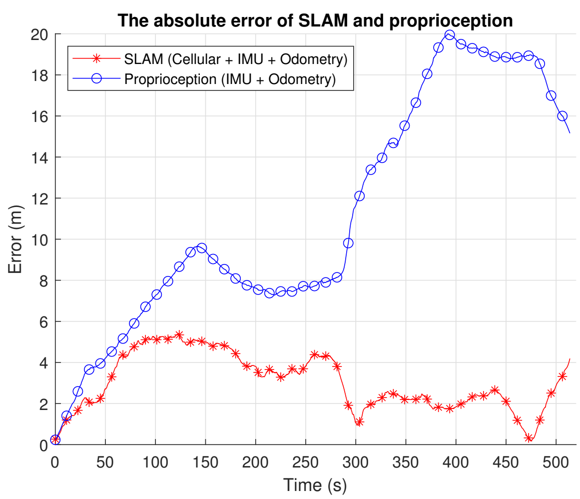

Fig. 4: The absolute error of SLAM and proprioception.

ACKNOWLEDGEMENT

This work was supported in part by the Swedish Innovation Agency VINNOVA through the MIMO-PAD Project (Reference number 2018-05000). Computational resources were provided by the Swedish National Infrastructure for Computing (SNIC) at HPC2N, partially funded by the Swedish Research Council through grant agreement no. 2018-05973.

REFERENCES

[1] E. Dahlman, S. Parkvall, and J. Skold, *5G NR: The Next Generation Wireless Access Technology*, 1st ed. USA: Academic Press, Inc., 2018.

[2] S. Dwivedi, R. Shreevastav, F. Munier, J. Nygren, I. Siomina *et al.*, "Positioning in 5G networks," *IEEE Communications Magazine*, vol. 59, no. 11, pp. 38–44, 2021.

[3] H. Wymeersch, D. Shrestha, C. M. de Lima, V. Yajnanarayana, B. Richerzhagen *et al.*, "Integration of communication and sensing in 6G: a joint industrial and academic perspective," in *Proc. IEEE 32nd Int. Symp. PIMRC*, 2021, pp. 1–7.

[4] Y. Ke, H. Gao, W. Xu, L. Li, L. Guo *et al.*, "Position prediction based fast beam tracking scheme for multi-user UAV-mmwave communications," in *ICC 2019 - 2019 IEEE International Conference on Communications (ICC)*, 2019, pp. 1–7.

[5] H. Bagheri, M. Noor-A-Rahim, Z. Liu, H. Lee, D. Pesch *et al.*, "5G NR-V2X: Toward connected and cooperative autonomous driving," *IEEE Communications Standards Magazine*, vol. 5, no. 1, pp. 48–54, 2021.

[6] S. Bartoletti, H. Wymeersch, T. Mach, O. Brunnegård, D. Giustiniano *et al.*, "Positioning and sensing for vehicular safety applications in 5G and beyond," *IEEE Communications Magazine*, vol. 59, no. 11, pp. 15–21, 2021.

[7] Z. Wang, L. Zhang, A. S. E. Edmonds, and S. Dang, "Network-based anti-theft alert system using dynamic hybrid TOA/AOA algorithm," *Journal of Communications*, vol. 11, no. 8, pp. 758–764, 2016.

[8] C. Laoudias, A. Moreira, S. Kim, S. Lee, L. Wirola *et al.*, "A survey of enabling technologies for network localization, tracking, and navigation," *IEEE Communications Surveys & Tutorials*, vol. 20, no. 4, pp. 3607–3644, 2018.

[9] Y. Bar-Shalom, P. Willett, and X. Tian, *Tracking and Data Fusion: A Handbook of Algorithms*. YBS Publishing, 2011.

[10] S. Thrun, W. Burgard, and D. Fox, *Probabilistic Robotics*, ser. Intelligent robotics and autonomous agents. The MIT Press, 2005.

[11] T. Fortmann, Y. Bar-Shalom, and M. Scheffe, "Sonar tracking of multiple targets using joint probabilistic data association," *IEEE Journal of Oceanic Engineering*, vol. 8, no. 3, pp. 173–184, 1983.

[12] D. Reid, "An algorithm for tracking multiple targets," *IEEE Transactions on Automatic Control*, vol. 24, no. 6, pp. 843–854, 1979.

[13] E. Leitinger, F. Meyer, F. Hlawatsch, K. Witrisal, F. Tufvesson *et al.*, "A belief propagation algorithm for multipath-based SLAM," *IEEE Transactions on Wireless Communications*, vol. 18, no. 12, pp. 5613–5629, Dec 2019.

[14] S. H. Rezatofighi, A. Milan, Z. Zhang, Q. Shi, A. Dick *et al.*, "Joint probabilistic data association revisited," in *2015 IEEE International Conference on Computer Vision (ICCV)*, 2015, pp. 3047–3055.

[15] M. Fromer and A. Globerson, "An LP view of the M-best MAP problem," *Advances in Neural Information Processing Systems*, vol. 22, 2009.

[16] J. Chen, R. Whiton, X. Li, and F. Tufvesson, "High-resolution channel sounding and parameter estimation in multi-site cellular networks," https://arxiv.org/abs/2211.09746, 2022.

[17] 3GPP, "Evolved Universal Terrestrial Radio Access (E-UTRA); Physical channels and modulation," 3rd Generation Partnership Project (3GPP), TS 36.211, Mar. 2017. [Online]. Available: http://www.3gpp.org/ftp/Specs/html-info/36211.htm

[18] P. Storms and F. Spieksma, "An LP-based algorithm for the data association problem in multitarget tracking," in *Proceedings of the Third International Conference on Information Fusion*, vol. 1, 2000, pp. TUD2/10–TUD2/16 vol.1.

[19] C. Gentner, T. Jost, W. Wang, S. Zhang, A. Dammann *et al.*, "Multipath assisted positioning with simultaneous localization and mapping," *IEEE Transactions on Wireless Communications*, vol. 15, no. 9, pp. 6104–6117, Sept 2016.

[20] A. Doucet, N. d. Freitas, K. P. Murphy, and S. J. Russell, "Rao-Blackwellised particle filtering for dynamic bayesian networks," in *Proc. Conf. Uncertainty in Artificial Intelligence*, ser. UAI '00. San Francisco, CA, USA: Morgan Kaufmann Publishers Inc., 2000, p. 176–183.

[21] E. W. Weisstein, "Euler angles," https://mathworld.wolfram.com/EulerAngles.html, online; accessed Dec 2022.

[22] S. M. Kay, *Fundamentals of Statistical Signal Processing: Estimation Theory*. Prentice Hall, 1997.